Quantum tunneling and evolution speed in an exactly solvable coupled double-well system

Hideo Hasegawa*

Department of Physics, Tokyo Gakugei University, Koganei, Tokyo 184-8501, Japan

(Dated: May 21, 2014)

arXiv:1403.0543v4 [quant-ph] 19 May 2014

Abstract

Exact analytical calculations of eigenvalues and eigenstates are presented for quantum coupled double-well (DW) systems with Razavy's hyperbolic potential. With the use of four kinds of initial wavepackets, we have calculated the tunneling period T and the orthogonality time τ which signifies a time interval for an initial state to evolve to its orthogonal state. We discuss the coupling dependence of T and τ, and the relation between τ and the concurrence C which is a typical measure of the entanglement in two qubits. Our calculations have shown that it is not clear whether the speed of quantum evolution may be measured by T or τ and that the evolution speed measured by τ (or T) is not necessarily increased with increasing C. This is in contrast with the earlier study [V. Giovannetti, S. Lloyd and L. Maccone, Europhys. Lett. **62** (2003) 615] which pointed out that the evolution speed measured by τ is enhanced by the entanglement in the two-level model.

Keywords: coupled double-well potential, Razavy's potential, concurrence, entanglement

PACS numbers: 03.65.-w, 03.67.Mn

*hideohasegawa@goo.jp

I. INTRODUCTION

Double-well (DW) potential models have been extensively employed in various fields of quantum physics, in which the tunneling is one of fascinating quantum effects. Although quartic DW potentials are commonly adopted for the theoretical study, one cannot obtain their exact eigenvalues and eigenfunctions of the Schrödinger equation. Then it is necessary to apply various approximate approaches such as perturbation and spectral methods to quartic potential models [1]. Razavy [2] proposed the quasi-exactly solvable hyperbolic DW potential, for which one may exactly determine a part of whole eigenvalues and eigenfunctions. A family of quasi-exactly solvable potentials has been investigated [3, 4].

The two-level (TL) system which is a simplified model of a DW system, has been employed for a study on qubits which play important roles in quantum information and quantum computation [5]. The relation between the entanglement and the speed of evolution of TL systems has been discussed [6–9]. The entanglement in qubits has been studied with the use of uncoupled and coupled TL models [8–10]. In recent years, several experimental studies for coupled TL systems have been reported [11, 12].

In contrast to the simplified TL model mentioned above, studies on *coupled* DW systems are scanty, as far as we are aware of. This is because a calculation of a coupled DW system is much tedious than those of a single DW system and of a coupled TL model. In the present study, we adopt coupled two DW systems, each of which is described by Razavy's potential. One of advantages of our model is that we may exactly determine eigenvalues and eigenfunctions of the coupled DW system. We study the tunneling period T and the orthogonality time τ which stands for the time interval for an assumed initial state to develop to its orthogonal state. We investigate the relation between the speed of quantum evolution measured by τ and the concurrence which is one of typical measures of entanglement of two qubits. The difference and similarity between results in our coupled DW system and the TL model [6–9] are discussed. These are purposes of the present paper.

The paper is organized as follows. In Sec. II, we describe the calculation method employed in our study, briefly explaining Razavy's potential [2]. Exact analytic expressions for eigenvalues and eigenfunctions for coupled DW systems are presented. In Sec. III, with the use of four kinds of initial wavepackets, we perform model calculations of tunneling period T and the orthogonality time τ. In Sec. IV, we discuss the relation between the calculated

τ and the concurrence. Sec. V is devoted to our conclusion.

II. THE ADOPTED METHOD

A. Coupled double-well system with Razavy's potential

We consider coupled two DW systems whose Hamiltonian is given by

$$H = \sum_{n=1}^{2}\left[-\frac{\hbar^2}{2m}\frac{\partial^2}{\partial x_n^2} + V(x_n)\right] - g x_1 x_2, \tag{1}$$

with

$$V(x) = \frac{\hbar^2}{2m}\left[\frac{\xi^2}{8}\cosh 4x - 4\xi\cosh 2x - \frac{\xi^2}{8}\right], \tag{2}$$

where x_1 and x_2 stand for coordinates of two distinguishable particles of mass m in double-well systems coupled by an interaction g, and $V(x)$ signifies Razavy's potential [2]. The potential $V(x)$ with $\hbar = m = \xi = 1.0$ adopted in this study is plotted in Fig. 1(a). Minima of $V(x)$ locate at $x_s = \pm 1.38433$ with $V(x_s) = -8.125$ and its maximum is $V(0) = -2.0$ at $x = 0.0$.

First we consider the case of $g = 0.0$ in Eq. (1). Eigenvalues of Razavy's double-well potential of Eq. (2) are given by [2]

$$\epsilon_0 = \frac{\hbar^2}{2m}\left[-\xi - 5 - 2\sqrt{4 - 2\xi + \xi^2}\right], \tag{3}$$

$$\epsilon_1 = \frac{\hbar^2}{2m}\left[\xi - 5 - 2\sqrt{4 + 2\xi + \xi^2}\right], \tag{4}$$

$$\epsilon_2 = \frac{\hbar^2}{2m}\left[-\xi - 5 + 2\sqrt{4 - 2\xi + \xi^2}\right], \tag{5}$$

$$\epsilon_3 = \frac{\hbar^2}{2m}\left[\xi - 5 + 2\sqrt{4 + 2\xi + \xi^2}\right]. \tag{6}$$

Eigenvalues for the adopted parameters are $\epsilon_0 = -4.73205$, $\epsilon_1 = -4.64575$, $\epsilon_2 = -1.26795$ and $\epsilon_3 = 0.645751$. Both ϵ_0 and ϵ_1 locate below $V(0)$ as shown by dashed curves in Fig. 1(a), and ϵ_2 and ϵ_3 are far above ϵ_1. In this study, we take into account the lowest two states of ϵ_0 and ϵ_1 whose eigenfunctions are given by [2]

$$\phi_0(x) = A_0\, e^{-\xi\cosh 2x/4}\left[3\xi\cosh x + (4 - \xi + 2\sqrt{4 - 2\xi + \xi^2})\cosh 3x\right], \tag{7}$$

$$\phi_1(x) = A_1\, e^{-\xi\cosh 2x/4}\left[3\xi\sinh x + (4 + \xi + 2\sqrt{4 + 2\xi + \xi^2})\sinh 3x\right], \tag{8}$$

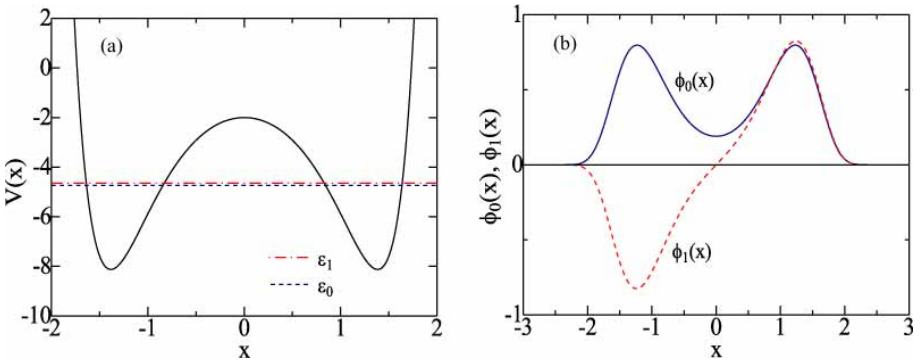

FIG. 1: (Color online) (a) Razavy's DW potential $V(x)$ (solid curve), dashed and chain curves expressing eigenvalues of ϵ_0 and ϵ_1, respectively, for $\hbar = m = \xi = 1.0$ [Eq.(2)]. (b) Eigenfunctions of $\phi_0(x)$ (solid curve) and $\phi_1(x)$ (dashed curve).

A_n $(n = 0, 1)$ denoting normalization factors. Figure 1(b) shows the eigenfunctions of $\phi_0(x)$ and $\phi_1(x)$, which are symmetric and anti-symmetric, respectively, with respect to the origin.

Figure 2(a) shows the 3D plot of the composite potential $U(x_1, x_2)$ defined by

$$U(x_1, x_2) \ = \ V(x_1) + V(x_2) - g x_1 x_2. \tag{9}$$

It has four minima of $U(\pm x_s, \pm x_s) = -16.25$ and one maximum of $U(0.0, 0.0) = -4.0$ for $g = 0.0$. Solid curves in Fig. 2(b) show contour plots of $U(x_1, x_2) = \mu$ for $\mu = -15$, -10 and -5 with $g = 0.0$. For a comparison, dashed curves shows the result with $g = 1.0$, for which $U(\pm x_s, \mp x_s) - U(\pm x_s, \pm x_s) = 3.8327$. Dashed curves with $g = 1.0$ are slightly different from solid curves with $g = 0.0$.

B. Eigenvalues and eigenstates of the coupled DW system

We calculate exact eigenvalues and eigenstates of the coupled two DW systems described by Eq. (1). With basis states of $\phi_0\phi_0$, $\phi_0\phi_1$, $\phi_1\phi_0$ and $\phi_1\phi_1$ where $\phi_n\phi_k \equiv \phi_n(x_1)\phi_k(x_2)$, the energy matrix for the Hamiltonian given by Eq. (1) is expressed by

$$\mathcal{H} \ = \ \begin{pmatrix} 2\epsilon_0 & 0 & 0 & -g\gamma^2 \\ 0 & \epsilon_0 + \epsilon_1 & -g\gamma^2 & 0 \\ 0 & -g\gamma^2 & \epsilon_0 + \epsilon_1 & 0 \\ -g\gamma^2 & 0 & 0 & 2\epsilon_1 \end{pmatrix}, \tag{10}$$

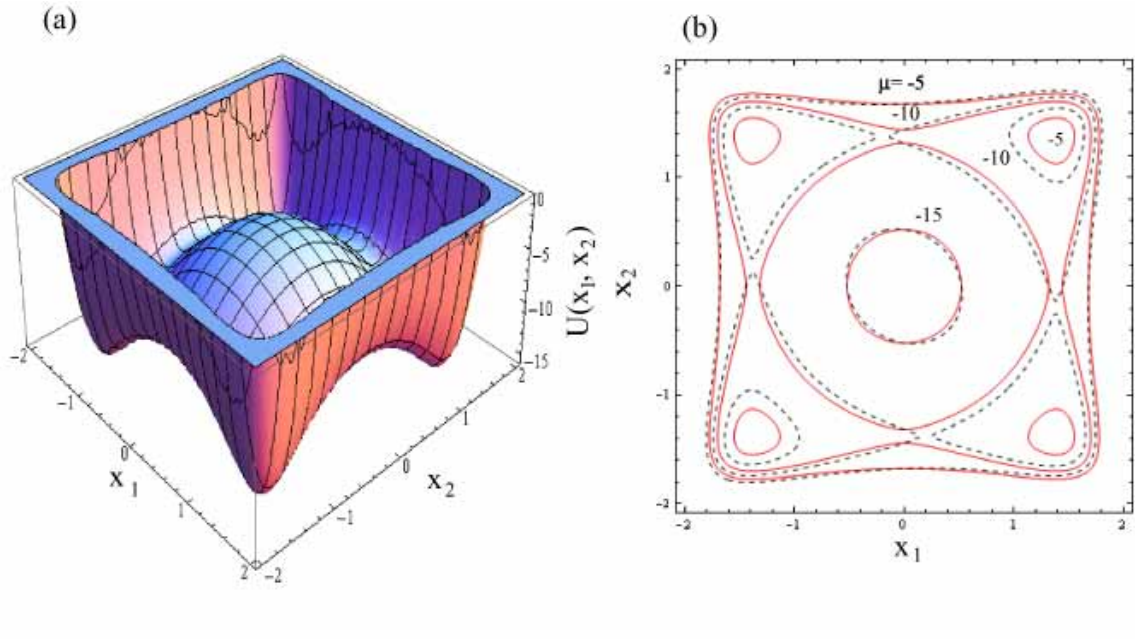

FIG. 2: (Color online) (a) 3D plot of a composite potential $U(x_1, x_2)$ as functions of x_1 and x_2. (b) Contour plots of $U(x_1, x_2) = \mu$ for $\mu = -15$, -10 and -5 with $g = 0.0$ (solid curves) and $g = 1.0$ (dashed curves).

with

$$\gamma \;=\; \int_{-\infty}^{\infty} \phi_0(x)\, x\, \phi_1(x)\, dx = 1.13823. \tag{11}$$

Eigenvalues of the energy matrix are given by

$$E_0 \;=\; \epsilon - \sqrt{\delta^2 + g^2\gamma^4}, \tag{12}$$

$$E_1 \;=\; \epsilon - g\gamma^2, \tag{13}$$

$$E_2 \;=\; \epsilon + g\gamma^2, \tag{14}$$

$$E_3 \;=\; \epsilon + \sqrt{\delta^2 + g^2\gamma^4}, \tag{15}$$

where

$$\epsilon \;=\; \epsilon_1 + \epsilon_0 = -9.3778, \tag{16}$$

$$\delta \;=\; \epsilon_1 - \epsilon_0 = 0.0863. \tag{17}$$

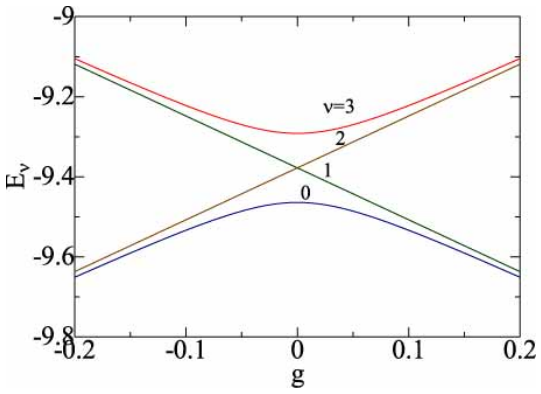

FIG. 3: (Color online) Eigenvalues E_ν ($\nu = 0{-}3$) of a coupled DW system as a function the coupling strength g.

Corresponding eigenfunctions are given by

$$\Phi_0(x_1, x_2) = \cos\theta\, \phi_0(x_1)\phi_0(x_2) + \sin\theta\, \phi_1(x_1)\phi_1(x_2), \tag{18}$$

$$\Phi_1(x_1, x_2) = \frac{1}{\sqrt{2}} \left[\phi_0(x_1)\phi_1(x_2) + \phi_1(x_1)\phi_0(x_2)\right], \tag{19}$$

$$\Phi_2(x_1, x_2) = \frac{1}{\sqrt{2}} \left[-\phi_0(x_1)\phi_1(x_2) + \phi_1(x_1)\phi_0(x_2)\right], \tag{20}$$

$$\Phi_3(x_1, x_2) = -\sin\theta\, \phi_0(x_1)\phi_0(x_2) + \cos\theta\, \phi_1(x_1)\phi_1(x_2), \tag{21}$$

where

$$\tan\, 2\theta = \frac{g\gamma^2}{\delta}. \quad \left(-\tfrac{\pi}{4} \le \theta \le \tfrac{\pi}{4}\right) \tag{22}$$

Eigenvalues E_ν ($\nu = 0$-3) are plotted as a function of g in Fig. 3, which is symmetric with respect to $g = 0.0$. For $g = 0.0$, E_1 and E_2 are degenerate. We hereafter study the case of $g \geq 0.0$. With increasing g, energy gaps between ϵ_0 and ϵ_1 and between ϵ_2 and ϵ_3 are gradually decreased while that between ϵ_1 and ϵ_2 is increased.

The time-dependent wavepacket is expressed by

$$\Psi(t) = \Psi(x_1, x_2, t) = \sum_{\nu=0}^{3} a_\nu\, \Phi_\nu(x_1, x_2)\, e^{-iE_\nu t/\hbar}, \tag{23}$$

where expansion coefficients a_ν satisfy the relation

$$\sum_{\nu=0}^{3} |a_\nu|^2 = 1. \tag{24}$$

Expansion coefficients a_ν may be formally determined for a given initial wavepacket, which requires cumbersome calculations. In this study they are assumed *a priori* as will be given shortly.

The correlation function $\Gamma(t)$ is defined by

$$\Gamma(t) \;=\; \Big| \int_{-\infty}^{\infty}\int_{-\infty}^{\infty} \Psi^*(x_1,x_2,0)\,\Psi(x_1,x_2,t)\,dx_1\,dx_2 \Big|, \tag{25}$$

$$\;=\; \Big| \,|a_0|^2 + \sum_{\nu=1}^{3} |a_\nu|^2\, e^{-i\Omega_\nu t} \Big|, \tag{26}$$

where $\Omega_\nu = (E_\nu - E_0)/\hbar$. The tunneling period T for the initial wavepacket given by Eq. (23) is determined by

$$T \;=\; \min_{\forall\, t>0} \{\Gamma(t) = 1\}. \tag{27}$$

On the contrary, the orthogonality time τ is provided by the time interval such that an initial wavepacket takes to evolve into the orthogonal state [6–9],

$$\tau \;=\; \min_{\forall\, t>0} \{\Gamma(t) = 0\}. \tag{28}$$

In the case of a simple wavepacket including only two states, *e.g.* $a_\nu = (1/\sqrt{2})(\delta_{\nu,0}+\delta_{\nu,\kappa})$, the correlation function becomes

$$\Gamma(t) \;=\; \frac{1}{2}|1 + e^{-i\Omega_\kappa t}| = \sqrt{\frac{1+\cos\Omega_\kappa t}{2}}, \tag{29}$$

for which we easily obtain T and τ

$$T \;=\; 2\tau = \frac{2\pi}{\Omega_\kappa}. \tag{30}$$

In the case of $g = 0.0$ where $\Omega_1 = \Omega_2 = \Omega_3/2$, Eqs. (27) and (28) become

$$T \;=\; \min_{\forall\, t>0} \{|a_0|^2 + (|a_1|^2 + |a_2|^2)\, z(t) + |a_3|^2\, z(t)^2 = 1\}, \tag{31}$$

$$\tau \;=\; \min_{\forall\, t} \{|a_0|^2 + (|a_1|^2 + |a_2|^2)\, z(t) + |a_3|^2 z(t)^2 = 0\}, \tag{32}$$

where $z(t) \;=\; e^{-i\Omega_1 t}$. Solutions of T and τ may be obtainable from roots of respective polynomial equations for $z(t)$ [8, 9].

In a general case, however, T and τ are obtained by solving Eqs. (27) and (28) with a numerical method, as will be shown later.

III. MODEL CALCULATIONS

Dynamical properties of wavepackets A-D with assumed expansion coefficients shown in Table 1, have been studied. We will report results of the case with $g = 0.0$ for wavepackets A and B in Sec. III A, and those with $g = 0.1$ for wavepackets C and D in Sec. III B.

wavepacket	a_0	a_1	a_2	a_3
A [Eq. (42)]	$\frac{1}{2}$	$\frac{1}{\sqrt{2}}$	0	$\frac{1}{2}$
B [Eq. (49)]	$\frac{1}{\sqrt{2}}$	0	0	$\frac{1}{\sqrt{2}}$
C [Eq. (54)]	$\frac{1}{\sqrt{2}}$	$\frac{1}{\sqrt{2}}$	0	0
D [Eq. (62)]	$\frac{1}{2}$	$\frac{1}{2}$	$\frac{1}{2}$	$\frac{1}{2}$

Table 1 Assumed expansion coefficients a_ν ($\nu = 0$ to 3) for four wavepackets A, B, C and D.

A. Uncoupled double-well system ($g = 0.0$)

First we consider the uncoupled DW with $g = 0.0$, for which eigenvalues are

$$E_0 \;=\; -9.4641, \quad E_1 = E_2 = -9.3778, \quad E_3 = -9.2915, \tag{33}$$

leading to

$$\Omega_1 \;=\; \Omega_2 = 0.0863, \quad \Omega_3 = 0.1726, \tag{34}$$

and eigenfunctions are given by

$$\Phi_0(x_1, x_2) \;=\; \phi_0(x_1)\phi_0(x_2), \tag{35}$$

$$\Phi_1(x_1, x_2) \;=\; \frac{1}{\sqrt{2}}\left[\phi_0(x_1)\phi_1(x_2) + \phi_1(x_1)\phi_0(x_2)\right], \tag{36}$$

$$\Phi_2(x_1, x_2) \;=\; \frac{1}{\sqrt{2}}\left[-\phi_0(x_1)\phi_1(x_2) + \phi_1(x_1)\phi_0(x_2)\right], \tag{37}$$

$$\Phi_3(x_1, x_2) \;=\; \phi_1(x_1)\phi_1(x_2). \tag{38}$$

Figure 4(a), 4(b), 4(c) and 4(d) show eigenfunctions $\Phi_\nu(x_1, x_2)$ for $\nu = 0$, 1, 2 and 3, respectively.

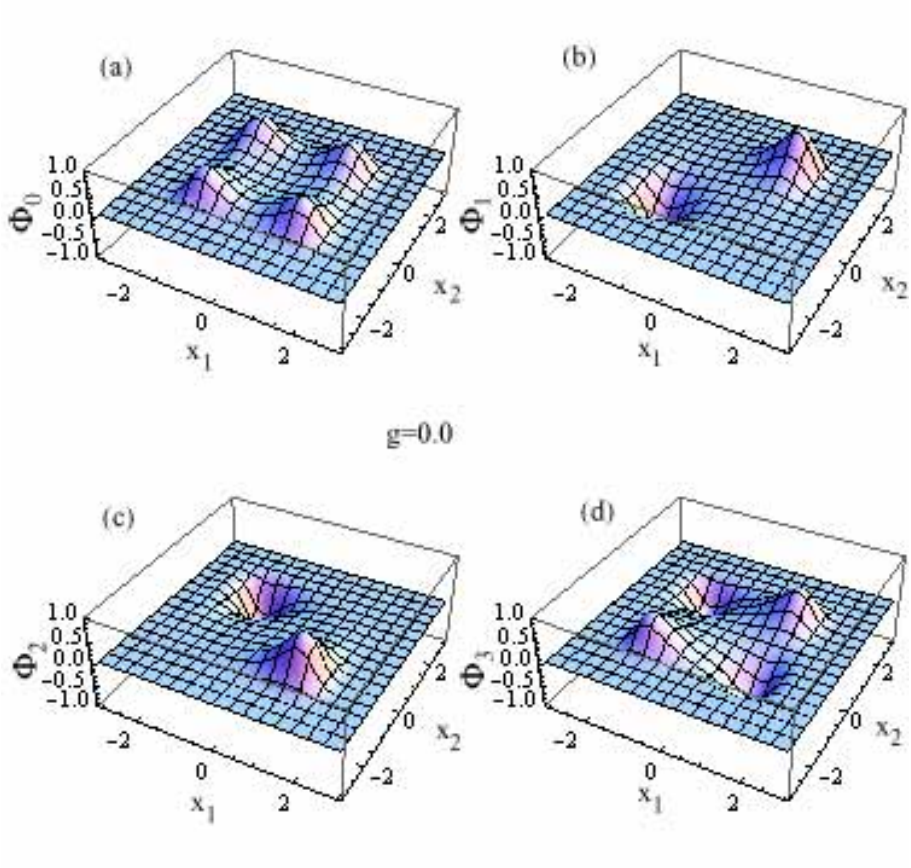

FIG. 4: (Color online) Eigenfunctions of (a) $\Phi_0(x_1, x_2)$, (b) $\Phi_1(x_1, x_2)$, (c) $\Phi_2(x_1, x_2)$, and (d) $\Phi_3(x_1, x_2)$ for $g = 0.0$.

1. Wavepacket A: $a_0 = 1/2$, $a_1 = 1/\sqrt{2}$, $a_2 = 0$ *and* $a_3 = 1/2$

A factorizable product state is expressed by

$$\Psi_{prod} = \Psi_{RR}(x_1, x_2) = \Psi_R(x_1)\Psi_R(x_2), \tag{39}$$

$$= \frac{1}{2}\left[\phi_0(x_1)\phi_0(x_2) + \phi_0(x_1)\phi_1(x_2) + \phi_1(x_1)\phi_0(x_2) + \phi_1(x_1)\phi_1(x_2)\right], \tag{40}$$

$$= \frac{1}{2}\left[\Phi_0(x_1, x_2) + \Phi_3(x_1, x_2)\right] + \frac{1}{\sqrt{2}}\Phi_1(x_1, x_2), \tag{41}$$

where magnitude of $\Psi_R(x_\nu)$ $(= [\phi_0(x_\nu) + \phi_1(x_\nu)]/\sqrt{2})$ localizes at the right well in the x_ν axis ($\nu = 1,\ 2$). The wavepacket yielding initially the product state given by Eq. (41) is described by

$$\Psi_A(x_1, x_2, t) = \frac{1}{2}\left[\Phi_0(x_1, x_2)\, e^{-iE_0 t/\hbar} + \Phi_3(x_1, x_2)\, e^{-iE_3 t/\hbar}\right] + \frac{1}{\sqrt{2}}\Phi_1(x_1, x_2)\, e^{-iE_1 t/\hbar}, \tag{42}$$

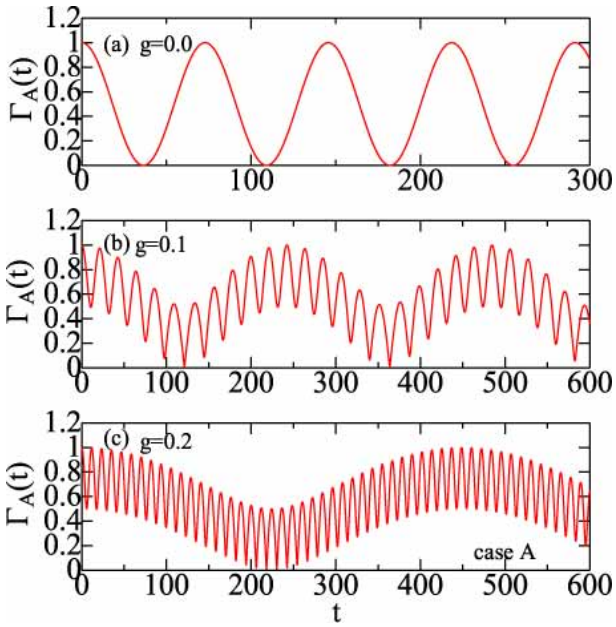

FIG. 5: (Color online) Correlation functions $\Gamma_A(t)$ with (a) $g = 0.0$, (b) $g = 0.1$ and (c) $g = 0.2$ for the wavepacket A.

and the relevant correlation function is given by

$$\Gamma_A(t) \;=\; |\frac{1}{4}\,\left(1+e^{-i\Omega_3 t/\hbar}\right)+\frac{1}{2}\,e^{-i\Omega_1 t}|, \tag{43}$$

where $\Omega_1 = \Omega_3/2 = 0.0863$. Calculated $\Gamma_A(t)$ is plotted in Fig. 5(a) which yields the tunneling period of $T = 2\pi/\Omega_1 = 72.81$ and the orthogonality time of $\tau = T/2 = 36.40$. Figures 5(b) and 5(c) will be explained later (Sec. IV B).

Time-dependent magnitudes of $|\Psi_A(x_1, x_2, t)|^2$ are shown in Figs. 6(a)-6(f). Figure 6(a) shows that the wavepacket initially has the maximum magnitude at the RR side of $(x_1, x_2) = (x_m, x_m)$ with $x_m = 1.23534$ near the bottom of the right-side well of $U(x_s, x_s)$ with $x_s = 1.38433$, where RR signifies the right side in the x_1 axis and the right side in x_2 axis. At $t = 0.2T$, $|\Psi_A(x_1, x_2, t)|^2$ in Fig 6(b) has finite magnitudes near LL, RL and LR sides besides RR one. This implies a tunneling of particles among four bottoms of $U(\pm x_s, \pm x_s)$. The orthogonal state to Eq. (41) is given by

$$\begin{aligned}
\Psi_{LL}(x_1, x_2) \;&=\; \Psi_L(x_1)\Psi_L(x_2), &(44)\\
&=\; \frac{1}{2}\left[\phi_0(x_1)\phi_0(x_2) - \phi_0(x_1)\phi_1(x_2) - \phi_1(x_1)\phi_0(x_2) + \phi_1(x_1)\phi_1(x_2)\right], &(45)\\
&=\; \frac{1}{2}\left[\Phi_0(x_1, x_2) + \Phi_3(x_1, x_2)\right] - \frac{1}{\sqrt{2}}\Phi_1(x_1, x_2), &(46)
\end{aligned}$$

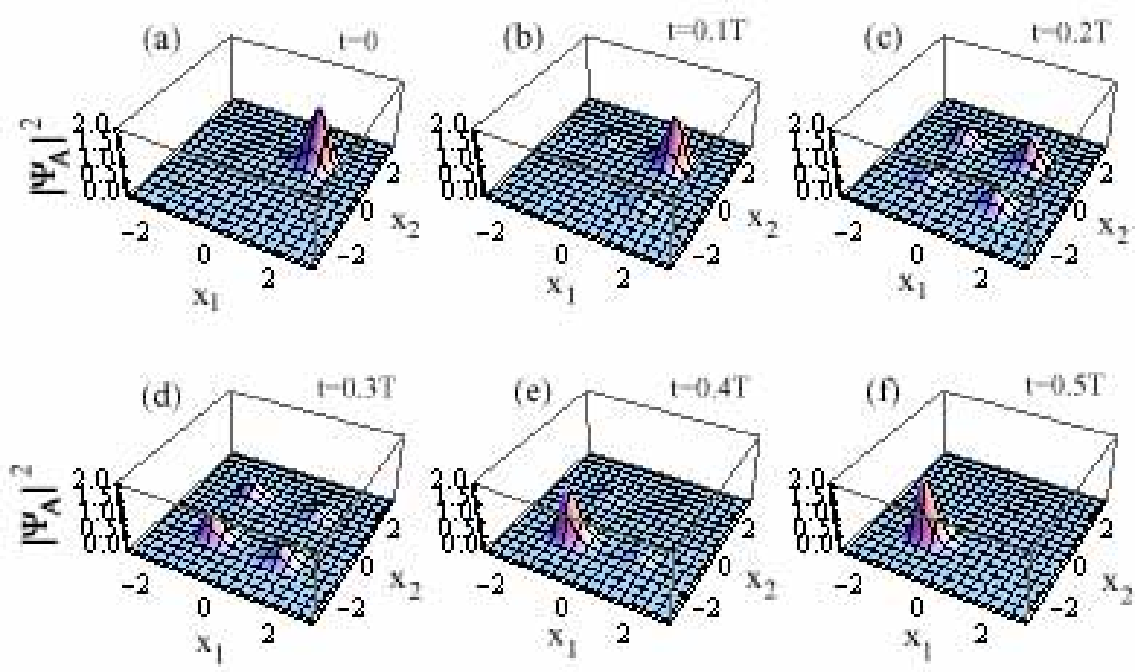

FIG. 6: (Color online) Time-dependent magnitudes of $|\Psi_A(x_1, x_2, t)|^2$ at (a) $t = 0.0$, (b) $t = 0.1T$, (c) $t = 0.2T$, (d) $t = 0.3T$, (e) $t = 0.4T$ and (f) $t = 0.5T$ for the wavepacket A [Eq.(42)] with $g = 0.0$ where $T = 72.81$. Magnitudes of wavepackets at $t = 0.6T$, $0.7T$, $0.8T$, $0.9T$ and T are the same as those at $t = 0.4T$, $0.3T$, $0.2T$, $0.1T$ and 0, respectively.

where magnitude of $\Psi_L(x_\nu)$ $(= [\phi_0(x_\nu) - \phi_1(x_\nu)]/\sqrt{2})$ localizes at the left well in the x_ν axis $(\nu = 1, 2)$. $\Psi_A(x_1, x_2, t)$ reduces to $\Psi_{LL}(x_1, x_2)$ at $t = 0.5T$, and it returns to $\Psi_{RR}(x_1, x_2)$ at $t = T$.

2. Wavepacket B: $a_0 = 1/\sqrt{2}$, $a_1 = a_2 = 0.0$ and $a_3 = 1/\sqrt{2}$

As a typical entangled state which cannot be expressed in a factorized form, we consider the state

$$\Psi_{ent}(x_1, x_2) = \frac{1}{\sqrt{2}} \left[\phi_0(x_1)\phi_0(x_2) + \phi_1(x_1)\phi_1(x_2)\right], \tag{47}$$

$$= \frac{1}{\sqrt{2}} \left[\Phi_0(x_1, x_2) + \Phi_3(x_1, x_2)\right]. \tag{48}$$

The relevant wavepacket is expressed by

$$\Psi_B(x_1.x_2, t) = \frac{1}{\sqrt{2}} \left[\Phi_0(x_1, x_2)\, e^{-iE_0 t/\hbar} + \Phi_3(x_1, x_2)\, e^{-iE_3 t/\hbar}\right], \tag{49}$$

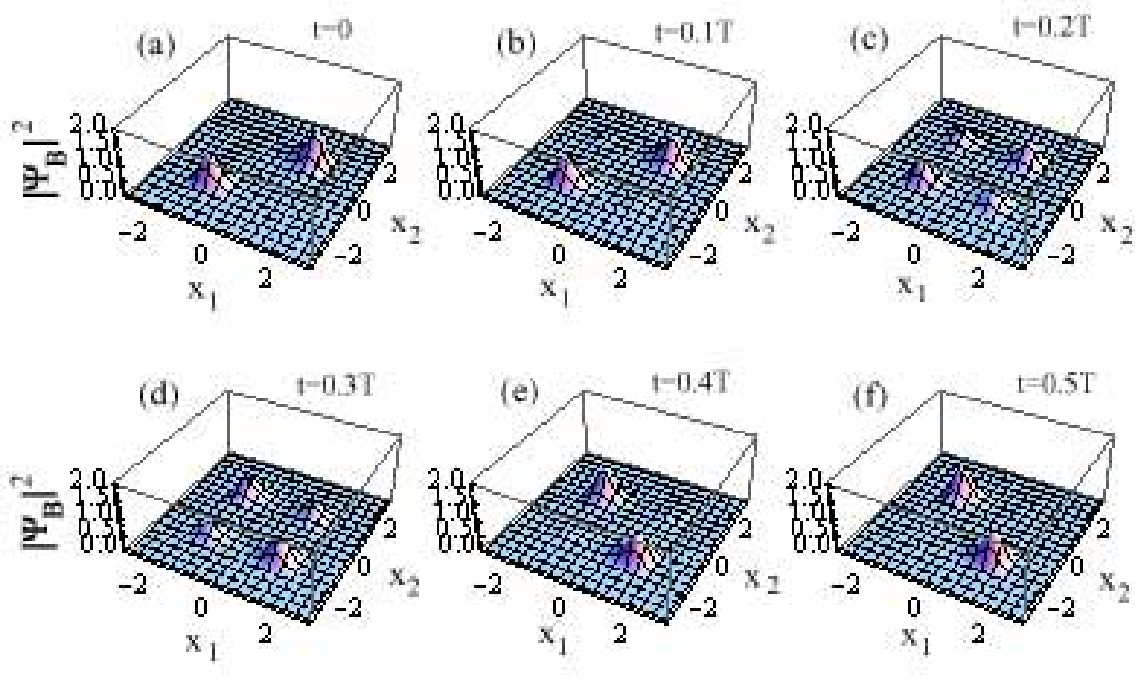

FIG. 7: (Color online) Time-dependent magnitudes of $|\Psi_B(x_1, x_2, t)|^2$ at (a) $t = 0.0$, (b) $t = 0.1T$, (c) $t = 0.2T$, (d) $t = 0.3T$, (e) $t = 0.4T$ and (f) $t = 0.5T$ for the wavepacket B [Eq.(49)] with $g = 0.0$ where $T = 36.40$.

and its correlation function is given by

$$\Gamma_B(t) \;=\; \frac{1}{2}|1 + e^{-i\Omega_3 t}| = \sqrt{\frac{1+\cos\Omega_3 t}{2}}, \tag{50}$$

where $\Omega_3 = 0.1726$. The tunneling period becomes $T = 2\pi/\Omega_3 = 36.40$ and the orthogonality time is given by $\tau = T/2 = 18.20$.

Figures 7(a)-7(f) show the time-dependent magnitudes of $|\Psi_B(x_1, x_2)|^2$ at $0 \le t \le T$. Initially $|\Psi_B(x_1, x_2)|^2$ has peaks at both RR and LL sides. At $t = 0.5T$, it reduces to

$$\Psi^{\perp}_{ent}(x_1, x_2) \;=\; \frac{1}{\sqrt{2}}\left[\Phi_0(x_1, x_2) - \Phi_3(x_1, x_2)\right], \tag{51}$$

which is orthogonal to the assumed initial state given by Eq. (48) and which has peaks at both RL and LR sides.

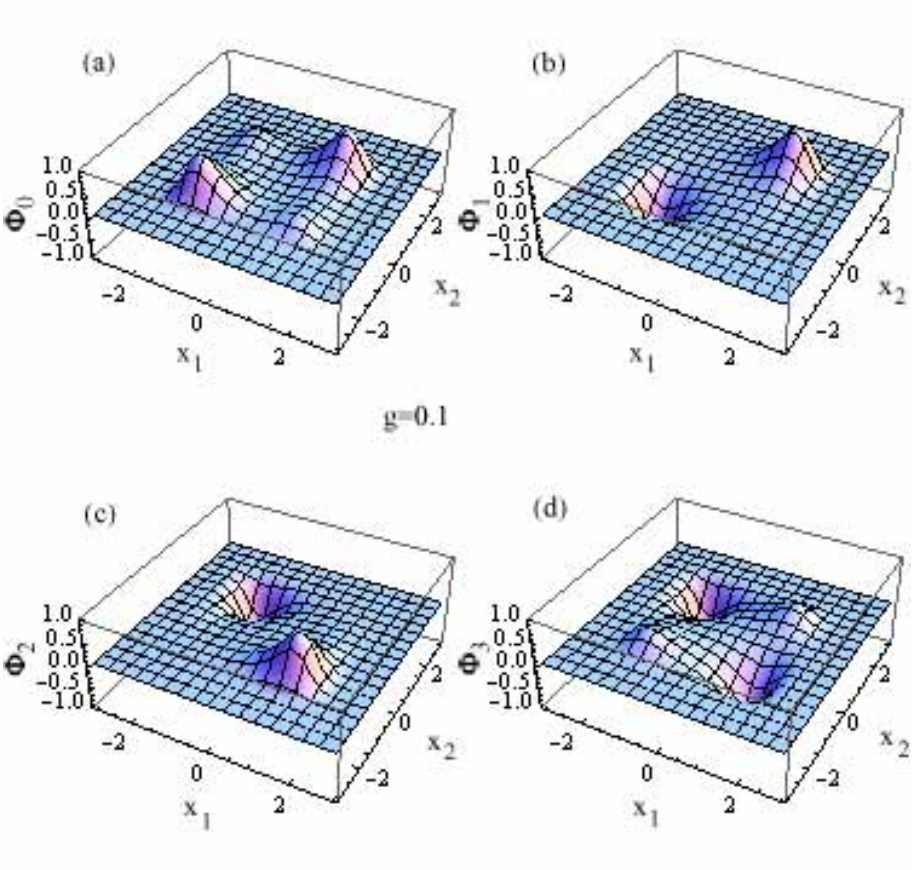

FIG. 8: (Color online) Eigenfunctions of (a) $\Phi_0(x_1, x_2)$, (b) $\Phi_1(x_1, x_2)$, (c) $\Phi_2(x_1, x_2)$, and (d) $\Phi_3(x_1, x_2)$ for $g = 0.1$.

B. Coupled double-well system ($g = 0.1$)

Next we study coupled DW systems with $g = 0.1$, for which eigenvalues are

$$E_0 \;=\; -9.53347, \;\; E_1 = -9.50736, \;\; E_2 = -9.24825, \;\; E_3 = -9.22213, \tag{52}$$

leading to

$$\Omega_1 \;=\; 0.02611, \;\; \Omega_2 = 0.28522, \;\; \Omega_3 = 0.31134. \tag{53}$$

The potential difference between the two bottoms is $U(\pm x_s, \mp x_s) - U(\pm x_s, \pm x_s) = 0.38327$. Figures 8(a)-8(d) show eigenfunctions $\Phi_\nu(x_1, x_2)$ for $\nu = 0 - 3$.

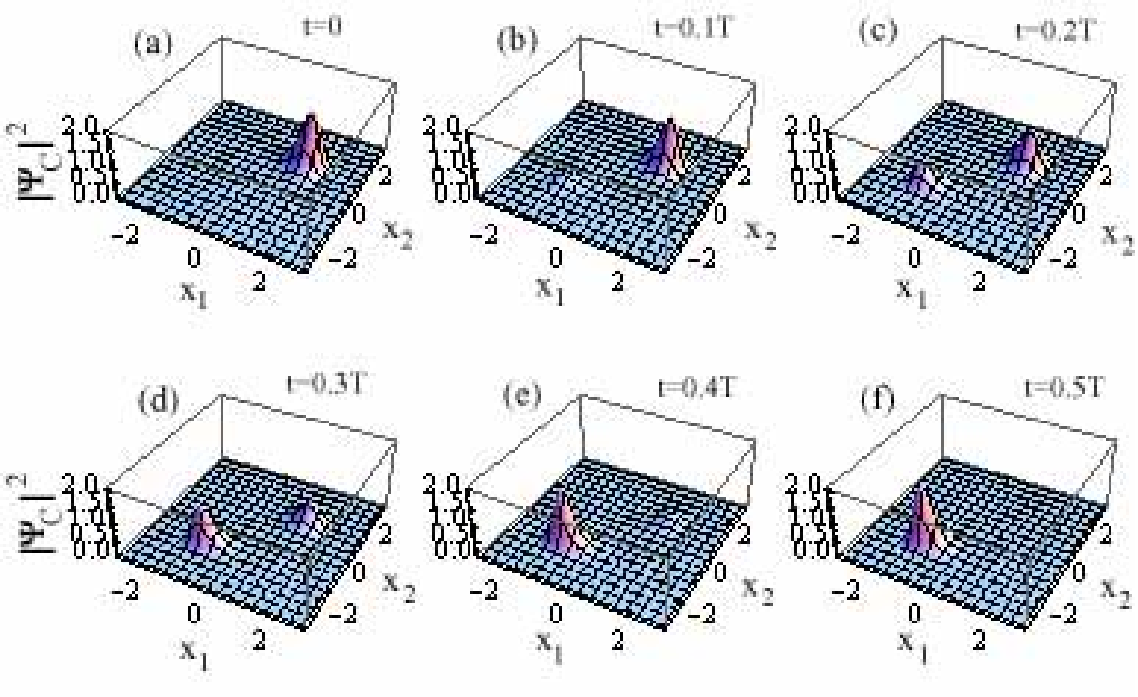

FIG. 9: (Color online) Time-dependent magnitudes of $|\Psi_C(x_1, x_2, t)|^2$ at (a) $t = 0.0$, (b) $t = 0.1T$, (c) $t = 0.2T$, (d) $t = 0.3T$, (e) $t = 0.4T$ and (f) $t = 0.5T$ for the wavepacket C [Eq. (54)] with $g = 0.1$ where $T = 240.63$.

1. Wavepacket C: $a_0 = a_1 = 1/\sqrt{2}$ *and* $a_2 = a_3 = 0$

With $a_0 = a_1 = 1/\sqrt{2}$ and $a_2 = a_3 = 0$, the wavepacket in Eq. (23) becomes

$$\Psi_C(x_1, x_2, t) \;=\; \frac{1}{\sqrt{2}} \left[\Phi_0(x_1, x_2)\, e^{-iE_0 t/\hbar} + \Phi_1(x_1, x_2)\, e^{-iE_1 t/\hbar} \right], \tag{54}$$

whose correlation function is given by

$$\Gamma_C(t) \;=\; \frac{1}{2} |1 + e^{-i\Omega_1 t}| = \sqrt{\frac{1 + \cos \Omega_1 t}{2}}, \tag{55}$$

with $\Omega_1 = 0.02611$. The tunneling period is $T = 2\pi/\Omega_1 = 240.63$ and the orthogonality time is $\tau = T/2 = 120.32$.

Figures 9(a)-9(f) show the time dependence of the magnitude of $|\Psi_C(x_1, x_2, t)|^2$. Figure 9(a) shows that at $t = 0$, the wavepacket given by

$$\Psi_C(x_1, x_2) \;=\; \frac{1}{\sqrt{2}} \left[\Phi_0(x_1, x_2) + \Phi_1(x_1, x_2) \right], \tag{56}$$

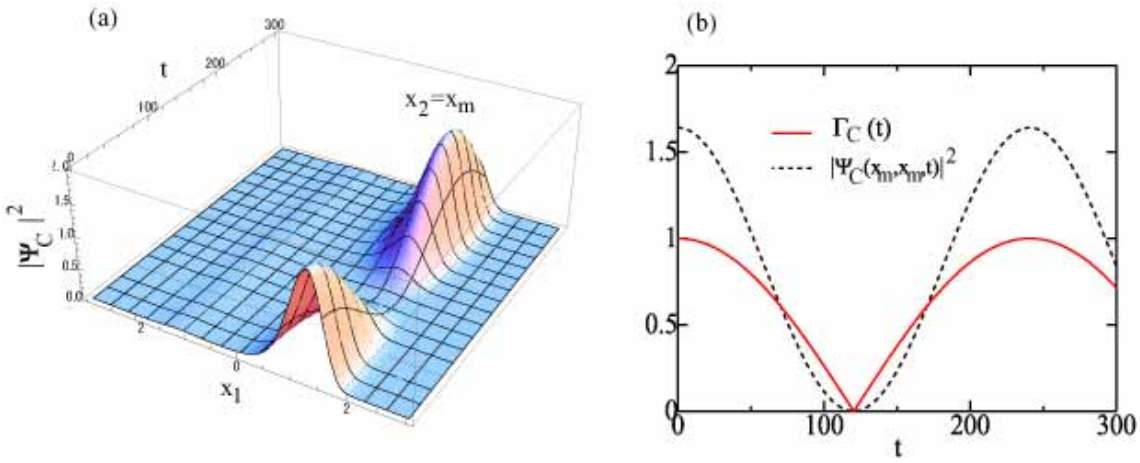

FIG. 10: (Color online) (a) 3D plot of $|\Psi_C(x_1, x_m, t)|^2$ as functions of x_1 and t with $x_m = 1.23534$. (b) Time dependence of $\Gamma_C(t)$ (solid curve) and $|\Psi_C(x_m, x_m, t)|^2$ (dashed curve) for the wavepacket C ($g = 0.1$).

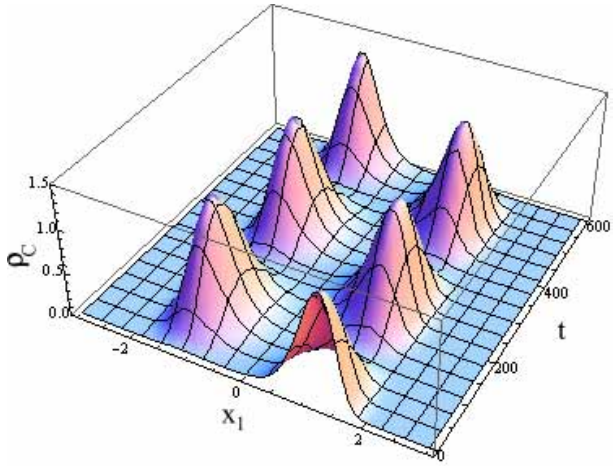

FIG. 11: (Color online) 3D plot of $\rho_C(x_1, t)$ as functions of x_1 and t for the wavepacket C ($g = 0.1$).

has the maximum magnitude at the RR side of $(x_1, x_2) = (x_m, x_m)$. We note that with time development, the magnitude of wavepacket at the initial position at the RR side is decreased while that at the LL side of $(x_1, x_2) = (-x_m, -x_m)$ is increased. At $t = 0.5T$, $\Psi_C(x_1, x_2, t)$ reduces to the state given by

$$\Psi_C^{\perp}(x_1, x_2) \;=\; \frac{1}{\sqrt{2}} \left[\Phi_0(x_1, x_2) - \Phi_1(x_1, x_2)\right], \tag{57}$$

whose magnitude locates at the LL side of $(x_1, x_2) = (-x_m, -x_m)$, and which is the orthog-

onal state to Eq. (56). This expresses the tunneling of a particle across the potential barrier at the origin of $(x_1, x_2) = (0.0, 0.0)$. The wavepacket returns to the initial state at $t = T$.

Dynamics of the wavepacket is studied in more detail. We show in Fig. 10(a), the 3D plot of $|\Psi_C(x_1, x_m, t)|^2$ as functions of x_1 and t. Solid and dashed curves in Fig. 10(b) show time dependences of $\Gamma(t)$ and $|\Psi_C(x_m, x_m, t)|^2$, respectively, which oscillate with a period of $T = 2\tau = 240.63$.

By using Eqs. (18)-(21) and (54), we calculate the density probability of the x_1 component

$$\rho_C(x_1, t) = \int_{-\infty}^{\infty} |\Psi_C(x_1, x_2, t)|^2 \, dx_2, \tag{58}$$

$$= \frac{1}{4}\left[(2\cos^2\theta + 1)\,\phi_0(x_1)^2 + (2\sin^2\theta + 1)\,\phi_1(x_1)^2\right] + \frac{1}{\sqrt{2}}(\cos\theta + \sin\theta)\,\phi_0(x_1)\phi_1(x_1)\,\cos\Omega_1 t. \tag{59}$$

The time-dependent expectation value of $\langle x_1 \rangle$ is expressed by

$$\langle x_1 \rangle = \int_{-\infty}^{\infty} \rho_C(x_1, t)\, x_1 \, dx_1, \tag{60}$$

$$= \frac{\gamma}{\sqrt{2}}\,(\cos\theta + \sin\theta)\,\cos\Omega_1 t, \tag{61}$$

where γ is given by Eq. (11). Figure 11 shows the 3D plot of $\rho_C(x_1, t)$. Similar analysis may be made for the component x_2. If we read $x_1 \to x_2$ in Fig. 11, it expresses the density probability for the x_2 component.

A comparison between Figs. 6(a) and 9(a) indicates that $\Psi_C(x_1, x_2, 0.0)$ is initially similar to $\Psi_A(x_1, x_2, 0.0)$, both of which have appreciable magnitudes at the RR site. Nevertheless, their time development is quite different: *e.g.* $\Psi_C(x_1, x_2, 0.2T) \neq \Psi_A(x_1, x_2, 0.2T)$.

2. Wavepacket D: $a_0 = a_1 = a_2 = a_3 = 1/2$

With $a_0 = a_1 = a_2 = a_3 = 1/2$, Eq. (23) yields the wavepacket given by

$$\Psi_D(x_1, x_2, t) = \frac{1}{2}\sum_{\nu=0}^{3} \Phi_\nu(x_1, x_2)\, e^{-iE_\nu t/\hbar}, \tag{62}$$

which leads to the correlation function

$$\Gamma_D(t) = \frac{1}{4}|1 + e^{-i\Omega_1 t} + e^{-i\Omega_2 t} + e^{-i\Omega_3 t}|, \tag{63}$$

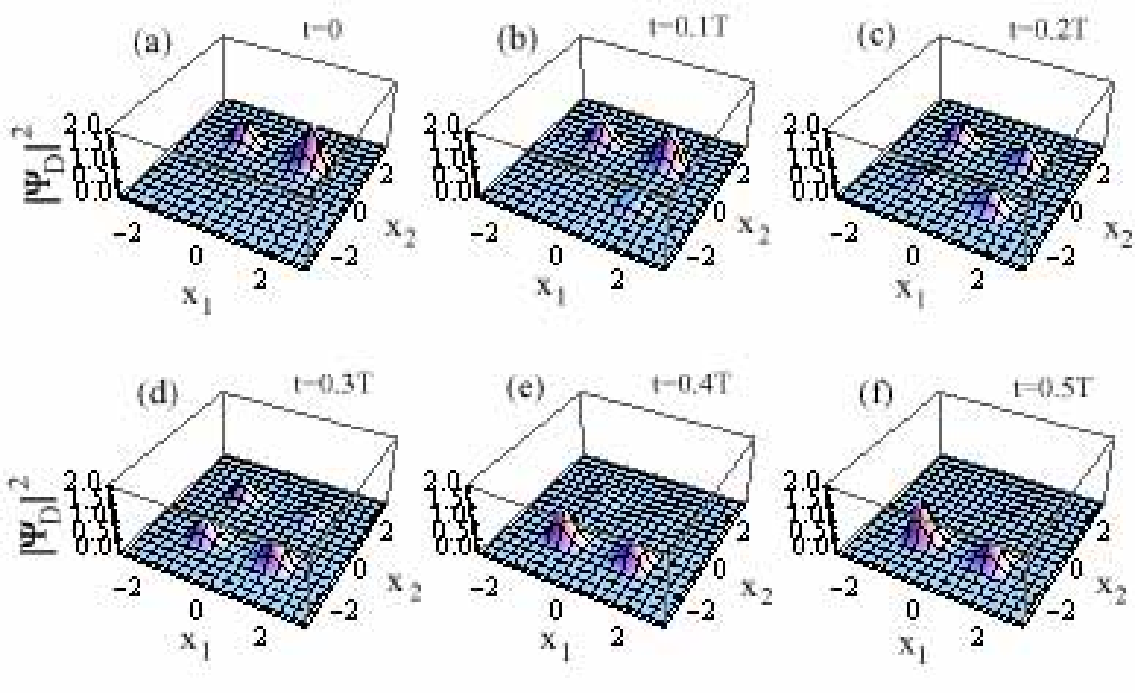

FIG. 12: (Color online) Time-dependent magnitudes of $|\Psi_D(x_1, x_2, t)|^2$ for (a) $t = 0$, (b) $t = 0.1T$, (c) $t = 0.2T$, (d) $t = 0.3T$, (e) $t = 0.4T$ and (f) $t = 0.5T$ for the wavepacket D [Eq. (62)] with $g = 0.1$ where $T = 242.32$.

with $\Omega_1 = 0.02611$, $\Omega_2 = 0.28522$ and $\Omega_3 = 0.31134$. The time-dependent $|\Psi_D(x_1, x_2, t)|^2$ from $t = 0$ to $t = 0.5T$ are shown in Figs. 12(a)-12(f) where $T = 242.32$ (below). In order to scrutinize its behavior, we show in Fig. 13(a), the 3D plot of $|\Psi_D(x_1, x_m, t)|^2$ as functions of x_1 and t. The dashed curve in Fig. 13(b) expresses $|\Psi_D(x_m, x_m, t)|^2$ whereas the solid curve shows $C_D(t)$ which is expressed as a superposition of three oscillations with frequencies of Ω_1, Ω_2 and Ω_3. Both $C_D(t)$ and $|\Psi_D(x_m, x_m, t)|^2$ show rapid and complicated oscillations with zeros of $C_D(t)$ at $t = 11.01\ (2k + 1)$ with $k = 0, 1, \cdots$. We obtain

$$T \ = \ 242.32 \simeq \frac{2\pi}{E_1 - E_0} = 240.63, \tag{64}$$

$$\tau \ = \ 11.01 \simeq \frac{\pi}{E_3 - E_1} = 11.02. \tag{65}$$

The tunneling period T is mainly determined by a energy gap between E_0 and E_1, while a small τ originates from a large energy gap between E_1 and E_3.

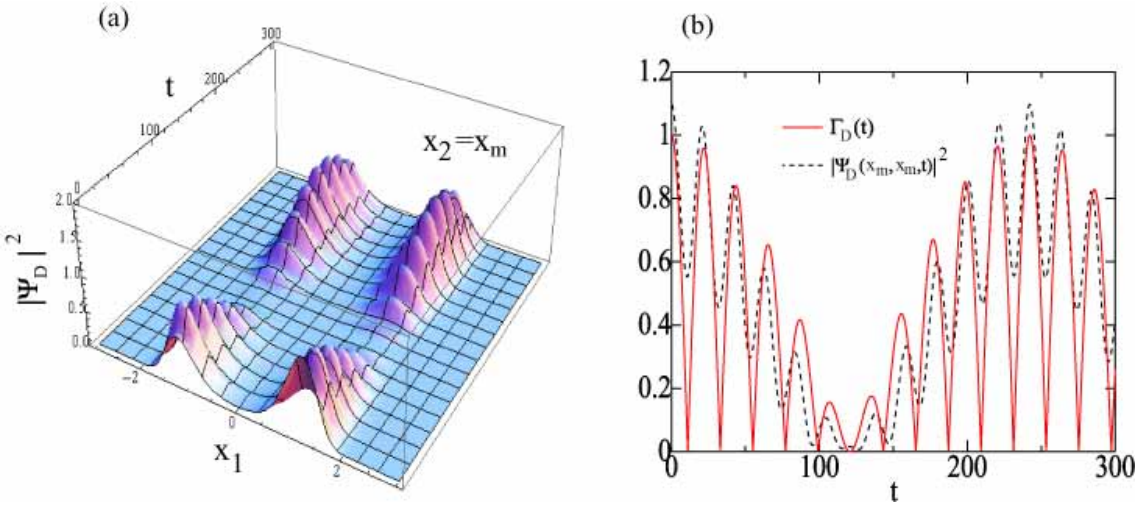

FIG. 13: (Color online) (a) 3D plot of $|\Psi_D(x_1, x_m, t)|^2$ as functions of x_1 and t with $x_m = 1.23534$. (b) Time dependence of $\Gamma_D(t)$ (solid curve) and $|\Psi_D(x_m, x_m, t)|^2$ (dashed curve) for the wavepacket D ($g = 0.1$).

IV. DISCUSSION

A. Comparison among results of four wavepackets A, B, C and D

It has been pointed out [6, 7] that the entanglement enhances the speed of evolution in certain quantum state as measured by the time speed to reach an orthogonal state. The orthogonality time τ is shown to be given by [6, 7]

$$\tau \geq \tau_{\min} \equiv \max\left(\frac{\pi\hbar}{2E}, \frac{\pi\hbar}{2\Delta E}\right), \tag{66}$$

where E and ΔE signify expectation and root-mean-square values, respectively, of the energy relative to E_0,

$$E = \sum_\nu |a_\nu|^2 (E_\nu - E_0), \tag{67}$$

$$\Delta E = \sqrt{\sum_\nu |a_\nu|^2 (E_\nu - E_0)^2 - E^2}. \tag{68}$$

Equations (66)-(68) show that the minimum orthogonality time τ_{min} depends on the distribution of eigenvalues and the expansion coefficient of wavepackets. Applying Eqs. (66)-(68) to our DW model in Eqs. (12)-(15), we have evaluated E, ΔE and τ_{min} whose results

are summarized in the Table 2. We note that τ_{min} is determined by E ($< \Delta E$) for the wavepacket C, while it is determined by ΔE ($< E$) for wavepackets A and D ($E = \Delta E$ for the wavepacket B).

The tunneling period T and the orthogonality time τ for four wavepackets A, B, C, and D calculated in the preceding section are summarized in Table 2. It is shown that τ in the four wavepackets are in agreement with results of $\tau \geq \tau_{min}$ evaluated by Eqs. (66)-(68). τ of the entangle wavepacket B is smaller than that of the non-entangled wavepacket A ($g = 0.0$), which is consistent with an enhancement of τ by entanglement in uncoupled qubits [6, 7].

wavepacket	g	T	τ	E	ΔE	τ_{min}	C
A	0.0	72.81	36.40	0.0863	0.0610	25.74	0.0
B	0.0	36.40	18.20	0.0863	0.0863	18.20	1.0
C	0.1	240.63	120.32	0.0131	0.1213	119.91	0.0839
D	0.1	242.32	11.02	0.1557	0.1432	10.97	0.2772

Table 2 The tunneling period T [Eq. (27)], the orthogonality time τ [Eq. (28)], the expectation value of the energy E [Eq. (67)], the root-mean-square value ΔE [Eq. (68)], the minimum orthogonality time τ_{min} [Eq. (66)], and the concurrence C [Eq. (72)] in four wavepackets A, B, C and D with couplings g (see Table 1).

B. Calculation of the concurrence

In order to examine the relation between τ_{min} and the entanglement, we have calculated the concurrence which is one of typical measures expressing the degree of entanglement. Substituting Eqs. (18)-(21) to Eq. (23) with $t = 0$, we obtain

$$|\Psi\rangle \;=\; c_{00}|0\;0\rangle + c_{01}|0\;1\rangle + c_{10}|1\;0\rangle + c_{11}|1\;1\rangle, \tag{69}$$

with

$$\begin{aligned} c_{00} \;&=\; a_0\,\cos\theta - a_3\,\sin\theta, \;\; c_{01} = \frac{1}{\sqrt{2}}(a_1 - a_2), \\ c_{10} \;&=\; \frac{1}{\sqrt{2}}(a_1 + a_2), \;\; c_{11} = c_0\,\sin\theta + a_3\,\cos\theta, \end{aligned} \tag{70}$$

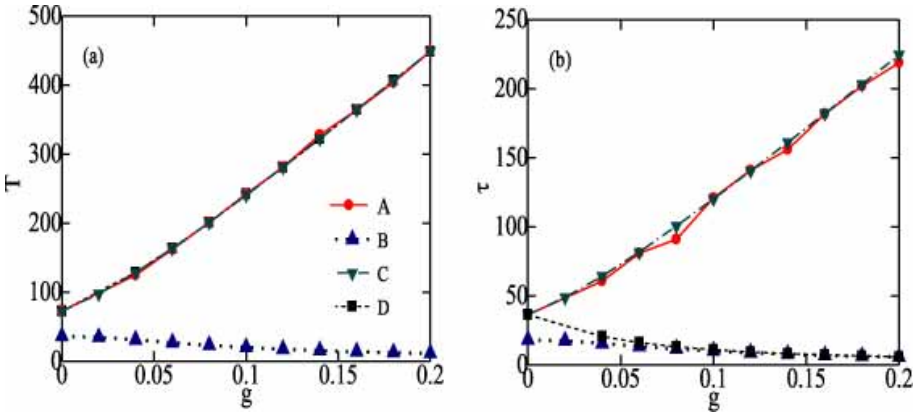

FIG. 14: (Color online) The g dependence of (a) the tunneling period T and (b) the orthogonality time τ for wavepacket A (circles), B (triangles), C (inverted triangles) and D (squares). Results of T for A, C and D are almost identical in (a).

where $|k\ \ell\rangle = \phi_k(x_1)\phi_\ell(x_2)$ with $k, \ell = 0, 1$. The concurrence C of the state $|\Psi\rangle$ given by Eq. (69) is defined by [13]

$$C \ = \ 2\,|c_{00}c_{11} - c_{01}c_{10}|. \tag{71}$$

The state given by Eq. (69) becomes factorizable if and only if the relation: $c_{00}c_{11} - c_{01}c_{10} = 0$ holds. Substituting Eq. (70) into Eq. (71), we obtain the concurrence

$$C \ = \ |(a_0^2 - a_3^2)\sin 2\theta + 2a_0a_3\cos 2\theta - a_1^2 + a_2^2|. \tag{72}$$

By using adopted coefficients in Table 1, we obtain the concurrence for the four wavepackets

$$C_A \ = \ \frac{1}{2}\,|1 - \cos 2\theta| \qquad \text{(wavepacket A)}, \tag{73}$$

$$C_B \ = \ |\cos 2\theta| \qquad \text{(wavepacket B)}, \tag{74}$$

$$C_C \ = \ \frac{1}{2}\,|1 - \sin 2\theta| \qquad \text{(wavepacket C)}, \tag{75}$$

$$C_D \ = \ \frac{1}{2}\,|\cos 2\theta| \qquad \text{(wavepacket D)}, \tag{76}$$

which lead to $C_A = 0.0$, $C_B = 1.0$ for $g = 0.0$ and to $C_C = 0.0839$ and $C_D = 0.2772$ for $g = 0.1$ (see Table 2).

C. The g dependence of T, τ, τ_{min} and C

So far calculations are reported only for wavepackets A and B with $g = 0.0$ and for wavepackets C and D with $g = 0.1$. We have calculated T, τ, τ_{min} and C, by changing g in a range of $0 \leq g < 0.2$ for four wavepackets A, B, C and D whose expansion coefficients a_ν ($\nu = 0 - 3$) are given in Table 1. For wavepackets B and C consisting of two terms, it is possible to exactly calculate the tunneling period and the orthogonality time with the use of Eq. (30). However, for wavepackets A and D with more than three terms, numerical methods are required for calculations of T and τ. Calculated T and τ are plotted in Figs. 14(a) and 14(b), respectively. Our calculations show that T and τ for the four wavepackets are given by

$$T_A \simeq T_C = \frac{2\pi}{E_1 - E_0}, \quad T_B = \frac{2\pi}{E_3 - E_0}, \quad T_D \simeq \frac{2\pi}{E_1 - E_0}, \tag{77}$$

$$\tau_A \simeq \tau_C = \frac{\pi}{E_1 - E_0}, \quad \tau_B = \frac{\pi}{E_3 - E_0}, \quad \tau_D \simeq \frac{\pi}{E_3 - E_1}, \tag{78}$$

where E_ν ($\nu = 0 - 3$) are g dependent [Eqs. (12)-(15)]. Figure 14(a) shows that with increasing g, the tunneling period is increased for wavepackets A, C and D while it is decreased for the wavepacket B. This is because a gap of $E_1 - E_0$ ($E_3 - E_0$) is decreased (increased) with increasing g (Fig. 3). Due to the similar reason, the orthogonality time for wavepackets A and C are increased with increasing g whereas it is decreased for wavepackets B and D, as shown in Fig. 14(b).

g dependences of τ_{min} and C calculated with the use of Eqs. (66)-(68) and Eqs. (73)-(76) for the four wavepackets are shown in Figs. 15(a)-15(d). Figure 15(a) shows that with increasing g for the wavepacket A, the concurrence is increased from a vanishing value of $C = 0.0$ at $g = 0.0$ while τ_{min} is decreased: a kink of τ_{min} at $g = 0.0366$ is due to a crossover of $\pi\hbar/2E = \pi\hbar/2\Delta E$ in Eq. (66). Figure 15(b) shows that for the wavepacket B, an increase in g induces a decrease in τ_{min} and C, the latter being decreased from the maximum concurrence of $C = 1.0$ at $g = 0.0$. For the wavepacket C, τ_{min} is increased but C is decreased with increasing g, as shown in Fig. 15(c). Figure 15(d) shows that both τ_{min} and C are decreased with increasing g for the wavepacket D.

Figures 16(a)-16(d) show T, τ and τ_{min} as a function of the concurrence C for the four wavepackets. It is shown that for a larger C, T is larger in wavepackets A and B, while it is smaller in wavepackets C and D. We note that for a larger concurrence, τ is larger

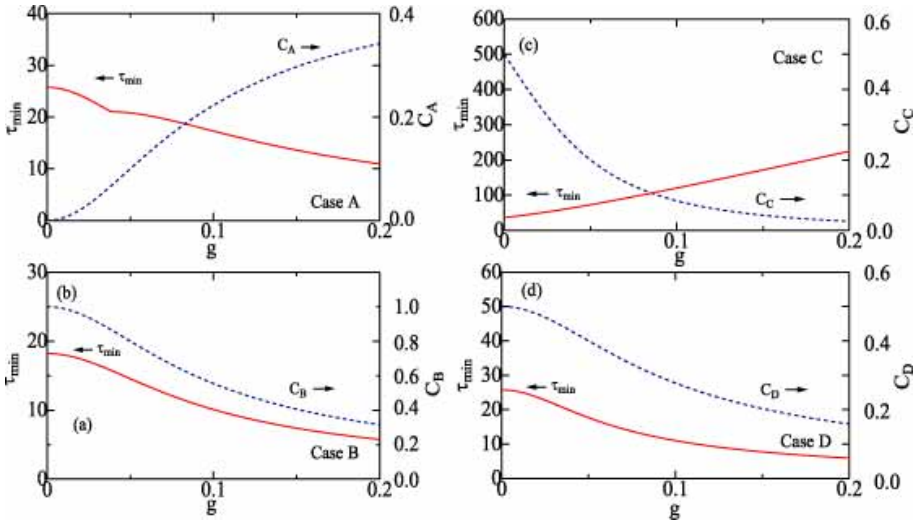

FIG. 15: (Color online) The minimum orthogonality time τ_{min} (solid curves) and the concurrence C (dashed curves) as a function of the interaction g for the wavepackets (a) A, (b) B, (c) C and (d) D, left and right ordinates being for τ_{min} and C, respectively.

for wavepackets A, B and D, but it is smaller for the wavepacket C. For a larger τ, T is larger in wavepackets A, B and C, but it is not the case for the wavepacket D. This fact imposes a question whether the evolution time may be measured by T or τ. Furthermore, the speed of quantum evolution measured by either τ or T is not necessarily increased when C is increased. This is in contrast with Refs. [6, 7] which claimed that the speed of a development of quantum state is improved by the entanglement. We also note that τ_{min} given by Eq. (66) provides us with fairly good estimates for lower limits of τ for wavepackets B, C and D. However, it does not for the wavepacket A. In order to clarify the point, we show the correlation functions $\Gamma_A(t)$ with $g = 0.0$, 0.1 and 0.2 for the wavepacket A in Figs. 5(a), 5(b) and 5(c), respectively. $\Gamma_A(t)$ with $g = 0.1$ and 0.2 more rapidly oscillates than that with $g = 0.0$. We obtain $(\tau, \tau_{min}) = (36.40,\ 25.74)$, $(121.00,\ 17.28)$ and $(218.77,\ 12.30)$ for $g = 0.0$, 0.1 and 0.2, respectively. With increasing g, τ is increased because of a narrowed energy gap of $E_1 - E_0$ in Eq. (78), whereas τ_{min} is decreased by a high-energy contribution of $E_3 - E_0$ in Eqs. (66)-(68). Although the relation: $\tau_{min} \leq \tau$ is actually held, the difference between τ and τ_{min} is significant with increasing g for the wavepacket A, where τ_{min} given by Eqs. (66)-(68) is not a good estimate of the lower bound of τ determined by Eq. (28).

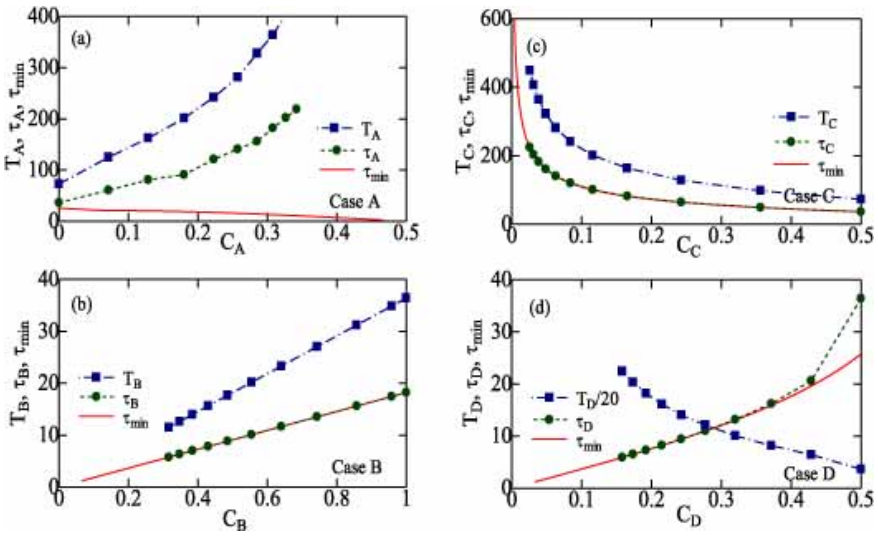

FIG. 16: (Color online) T (chain curves), τ (dashed curve) and τ_{min} (solid curves) as a function of the concurrence C for wavepackets (a) A, (b) B, (c) C and (d) D, T in (d) being divided by a factor of 20.

V. CONCLUSION

With the use of an exactly solvable coupled DW system described by Razavy's potential [2], we have studied the dynamics of four wavepackets A, B, C and D (Table 1). Our calculations of tunneling period T and the orthogonality time τ yield the followings:

(1) Although the relation: $T = 2\tau$ holds for wavepackets B and C including two terms, it is not the case in general. In particular for the wavepacket D, T is increased but τ is decreased with increasing g (Fig. 14), and

(2) g dependences of T and τ considerably depend on a kind of adopted wavepackets (Fig. 14), and they are increased or decreased with increasing the concurrence, depending on an initial wavepacket (Figs. 15 and 16).

A query arises from the item (1) whether the speed of a quantum evolution may be measured by T or τ, although it is commonly evaluated by τ [6–10]. The item (2) implies that even if the evolution speed is measured by either τ or T, it is not necessarily increased by the entanglement. This is in contrast with Refs. [6–10] which pointed out an enhancement of the evolution speed by the entanglement in TL models. The difference between their results and ours arises from the fact that the coupled DW model has much freedom than

the TL model: the latter is a simplified model of the former. It would be interesting to experimentally observed the time-dependent magnitude of $|\Psi(x_1, x_2, t)|^2$, which might be possible with advanced recent technology. In the present study, we do not take into account environmental effects which are expected to play important roles in real DW systems. An inclusion of dissipative effects is left as our future subject.

Acknowledgments

This work is partly supported by a Grant-in-Aid for Scientific Research from Ministry of Education, Culture, Sports, Science and Technology of Japan.

---

[1] D. J. Tannor, *Introduction to quantum mechanics: A time-dependent perspective* (Univ. Sci. Books, Sausalito, California, 2007).

[2] M. Razavy, Am. J. Phys. **48** (1980) 285.

[3] F. Finkel, F. Finkel, A. Gonzalez-Lopez and M. A. Rodriguez, J. Phys. A **32** (1999) 6821.

[4] B. Bagchi and A. Ganguly, arXiv:0302040.

[5] M. J. Storcz and F. K. Wilhelm, Phys. Rev. A **67** (2003) 042319.

[6] V. Giovannetti, S. Lloyd, and L. Maccone, Europhys. Lett. **62** (2003) 615.

[7] V. Giovannetti, S. Lloyd, and L. Maccone, Phys. Rev. A **67** (2003) 052109.

[8] J. Batle, M. Casas, A. Plastino, and A. R. Plastino, Phys. Rev. A **72** (2005) 032337.

[9] S. Curilef, C. Zander and A. R. Plastino, Eur. J. Phys. **27** (2006) 1193.

[10] C. Zander, A. Borras, A. R. Plastino, A. Plastino, and M. Casas, J. Phys. A **46**, 095302 (2013).

[11] Yu. A. Pashkin, T. Yamamoto, O. Astafiev, Y. Nakamura, D. V. Averin, and J. S. Tsai, Nature **421** (2003) 823.

[12] J. B. Majer, F. G. Paauw, A.C. J. ter Haar, C. J. P.M. Harmans, and J. E. Mooij, Phys. Rev. Lett. **94**, 090501 (2005).

[13] W. K. Wootters, Quan. Inf. Comp. **1** (2001) 27.